SIMULATION STUDY ON THE PERFORMANCE OF SOLAR AND GEOTHERMAL HYBRID R22 HEAT PUMP

Byun Kang[1], Jae-Kyeong OH[2], Cha-Sik Park[3] , and HongHyun Cho[4]

[1] Graduate school of Mechanical Engineering / Chosun University, Kwangju 501-759 (korea)

[2] Graduate school of Mechanical Engineering / Chosun University, Kwangju 501-759 (korea)

[3] Department automotive Engineering / Hoseo University, Asan 336-795 (korea)

[4] Department Mechanical Engineering / Chosun University, Kwangju 501-759 (korea)

ABSTRACT

A simulation study on the performance of the solar and geothermal hybrid heat pump system by using R22 was carried out with a variation of operating conditions. The system was consisted of solar system (concentric evacuated tube solar collector, heat storage tank) and geothermal heat pump system (double pipe heat exchanger, electric expansion valve and compressor). As a result, the heating capacity is linearly decreased from 13.2 kW to 11 kW as the heat pump operating temperature increases from 40°C to 48°C. Besides, the heating COP decreases by 13.6% from 4.4 to 3.8 when the ground temperature raises 13°C to 17°C. The heating capacity is increased by 4.7% from 11.5 kW to 12.2 kW and the heating COP rises by 19% from 4.7 to 5.6.

KEYWORKDS

Heat pump, R22, COP, Hybrid, Solar, Geothermal

NOMENCLATURE

A	area (m^2)
c_1-c_5	coefficients in eq. (6)
D	diameter (m)
F_R	collector heat removal factor
$F_R\tau\alpha$	intercept of the efficiency curve
h	enthalpy (KJ kg^{-1})
I_t	solar radiation (W/m^2)
L	length in EEV (m)
$\dot{m}$	mass flow rate (kg/s)
N	RPM
$\bar{S}_p$	Relative piston stroke length
P	pressure (kPa)
T	temperature (°C)
T_i	inlet temperature at the collector (°C)
T_a	outlet temperature at the collector (°C)
U_L	collector overall heat loss coefficient

V_{comp}	compressor volume (kg/m^3)
V_s	compressor inlet volume (kg/m^3)
W	compressor work (kW)
ρ	density (kg/m^3)
ε	compression ratio

1. INTRODUCTION

Recently, awareness of the effect of human activities on the environment and the developing debate on climate change has heightened and interested in non-fossil energy source. Since the limitation of energy usage and energy crisis became the problem in the world, the necessity of developing new energy resources has been a hot issue for the whole world in related to an alternative energy. Among the renewable energy, solar energy has advantages such as the cheaper maintain cost, clean and limitless. However, solar energy has serious problems like the low density solar energy, the impact of climate change and unstable energy supplies. To solve these problems, solar and geothermal hybrid heat pump system has been developed in this study. As solar radiation is enough, solar and geothermal hybrid heat pump system absorbed solar energy by solar collection. On the other hand, when the solar radiation is not enough to operate, the required energy can be filled by using heat pump. Besides, geothermal heat pump system can be used a constant temperature for year. Furthermore, the energy usage could be decreased by using this system for all season. In this study, a heat pump model with solar and geothermal heating system for residentail heating was developed. For efficient use of the solar and geothermal hybrid heat pump an optimal operation control emthod is required in order to save enery and increase reliablility. To address these problem, the performance date of the solar and geothermal hybird heat pump system have been analysed against the pump operating temperature and goethermal temperature.

2. SYSTEM MODELING

The solar and geothermal hybrid heat pump system (SG-HHPS) consists of a solar heat system and a geothermal heat pump system used refrigerant R22. The solar heat system has a concentric evacuated tube collector and a heat storage tank. The geothermal heat pump system consists of two double-pipe heat exchangers (high- & low-temp), a double pipe type evaporator, an EEV (electric expansion valve) and a compressor. For modeling of system components and calculating of thermodynamic refrigerant properties, EES (engineering equation solver) is used. A schematic diagram of the SG-HHPS used in this study is shown in Fig.1.

2.1 Solar collector and heat storage tank modeling

The solar collector has eight concentric evacuated tube collectors which can be reliably operated for getting heat for residential application. As a working fluid water-propylene glycol mixture (water to propylene glycol ratio of 80:20) is used. The solar collector model was developed based on test results of the concentric evacuated tube collector by Korean Institute of Energy Research. In this study, the efficiency of solar collector is calculated by eq.(1).

$$\eta_{collector} = F_R\tau\alpha - F_R U_L \left[\frac{(ti-ta)}{I_T}\right] = 0.7410 - 2.7469 \left[\frac{(ti-ta)}{I_T}\right] \qquad \text{(eq. 1)}$$

Solar hybrid systems show some dependability problems because of the time lag when solar energy is acquired and when it is used. To solve this problem, the heat storage tank (1.0 ton) was designed, and total collection heat was calculated by eq.(2).

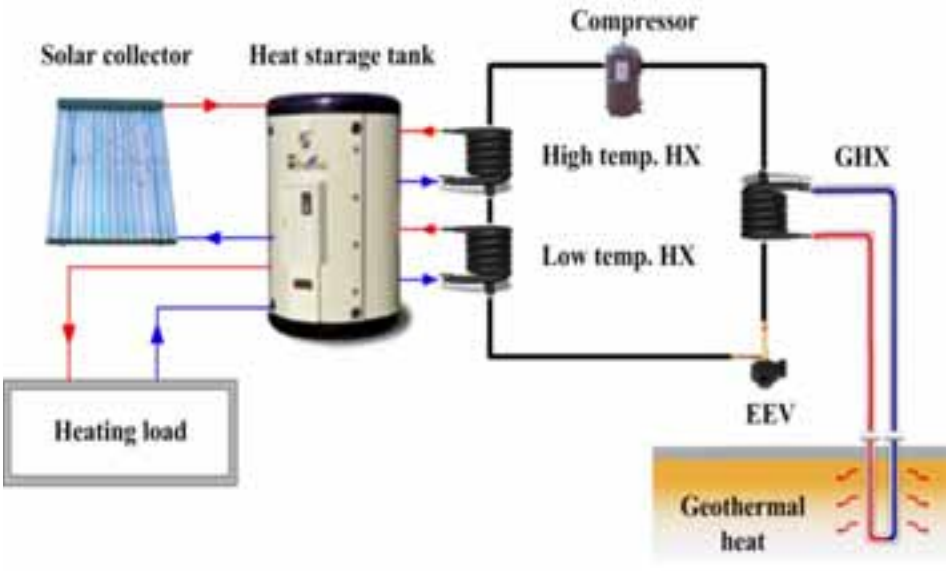

Fig. 1: Schematic diagram of the SG-HHPS (solar and geothermal hybrid heat pump system)

$$\int_j^{j+1} Q_{storage} = \int_0^j Q_{storage} + \int_0^j Q_{collector} + \int_0^j Q_{heat\ pump} - \int_0^j Q_{hotwater} - \int_0^j Q_{heating} \quad \text{(eq. 2)}$$

2.2 Compressor modeling

The reciprocating type compressor used for the simulation analysis used as the heat pump system of using R22 for developing the analytical model. In addition to, the mass flow rate of the compressor was calculated by using volumetric efficiency and isentropic efficiency, respectively.

$$\dot{m} = V_{comp} N \frac{\eta_v}{V_s} \quad \text{(eq. 3)}$$

$$\eta_v = 0.3596 + 1.1072\bar{S}_p - 0.08132\varepsilon + 0.0001175N - 0.4025\bar{S}_p^2 - 2.449\times10^{-8}N^2 \quad \text{(eq. 4)}$$

$$\eta_i = 0.2402 + 1.4187\bar{S}_p - 0.09698\varepsilon + 0.000123N - 0.5852\bar{S}_p^2 - 2.457\times10^{-8}N^2 \quad \text{(eq. 5)}$$

2.3 Heat exchanger modeling

The heat pump system consists of three double-pipe heat exchanger (high & low temperature condenser and evaporator), an EEV (electric expansion valve), and a reciprocating type compressor. In the heating mode, the double-pipe heat exchanger acts as an evaporator to exchange heat between the refrigerant and water that is supplied from the GHX (ground heat exchanger). And two double-pipe heat exchangers play the role of the condenser. The high temperature heat exchanger is placed at the compressor outlet. It exchanges the heat from high-temperature water to the middle of the heat storage tank so as to supply the hot water to the user. The low temperature double-pipe heat exchanger exchanges the heat from low-temperature water at the bottom of heat storage tank to supply the mean temperature water for heating. Table 1 shows property reference data for heat exchanger simulation used in this study.

2.4 EEV modeling

The EEV with a diameter of 1.6 mm is used as an expansion device so as to calculate the mass flow rate

Tab. 1: Property references for simulation

	Type	Refrigerant heat transfer coefficient	Refrigerant pressure drop	Water transfer coefficient
Condenser	Double pipe	Gnielinski (1976)	Churchill (1977)	Dittus and Boelter (1985)
Evaporator		Shah (1979)	Churchill (1977)	

through the expansion device. In this study, the expansion process is assumed to be isenthalpic. The mass flow rate of the EEV is calculated by using 6-physical and 4-geometrical variables based on Buckingham-π theory as shown below in eq. (6). The constants of eq. (6) are shown in Table 2.

$$\left(\frac{\dot{m}}{A_{t,m}\sqrt{\rho\Delta P}}\right) = C_1 \left(\frac{L}{D_m}\right)^{C_2} \left(\frac{D_m}{D_o}\right)^{C_3} \left(\frac{P_{in}}{P_c}\right)^{C_4} \left(\frac{T_{in}}{T_C}\right)^{C_5} \quad \text{(eq. 6)}$$

Tab. 2: Constants in EEV correlation of eq. (6)

Constant	Value
C_1	1.17×10^{0}
C_2	3.99×10^{-2}
C_3	-7.27×10^{-2}
C_4	3.86×10^{-1}
C_5	-4.55×10^{0}

2.5 Simulation conditions

To simulate heating load, the indoor space of 66.25 m^2 was assumed. The heat loss on inner walls was ignored, but losses on roof and outside walls with windows have been considered. Besides, the daily usage of the hot water was assumed to be 280*L* for four-member family according to ASHRAE standard 116 (1983). The design parameters of heating load and hot water load are shown in Tables 3 and 4. In this study, the performance analysis of the SG-HCHP system with heat pump operating temperature was carried out in order to compare the performance characteristics. The heat pump operating temperature means the setting temperature that can supply the heat to heat storage tank by the heat pump when the water temperature is reduced below the designed temperature. Simulation conditions used in this study are shown in Table 5.

Tab. 3: Heating load design

Parameters	Conditions
Indoor space	65.25 m^2
Thermal conductivity (W/m°C)	Brick: 0.53 Styrofoam: 0.02 Glass: 0.5
Windows (cm)	90×170×1.5 cm Glass 8 EA
Wall (cm)	Brick : 15 cm Styrofoam: 5 cm
Roof (cm)	Brick: 20 cm

Tab. 4: Hot water load design

Time	Usage water (L)
09 : 00	100
13 : 00	80
18 : 00	100

Tab. 5: Simulation conditions

Parameter	Conditions
Heat pump operating temp. (°C)	40, 42, 44, 46, 48
Ground temp. (°C)	11, 13, 15, 17, 19

3. RESULTS AND DISCUSSION

3.1The effect of heat pump operating temperature on system performance

Fig. 2 shows the variations of the optimal EEV opening, mass flow rate, heating capacity, and COP with heat pump operating temperature. The heating capacity is proportionally decreased from 13.2 kW to 11 kW as the heat pump operating temperature increases from 40^{o}C to 48^{o}C. Besides, the heating COP decreases by 13.6% from 4.4 to 3.8 EEV opening of the heat pump is one of the most important control factors to determine system performance because it affects the mass flow rate of the refrigerant and the compressor discharge pressure. In this study, when the heat pump operating temperature increase from 40^{o}C to 48^{o}C, the optimal EEV opening decreases from 46% to 40%, and mass flow rate decreases from 76 g/s to 65 g/s.

Fig. 3 shows the variations of the compressor work, pressure ratio, condenser outlet temperature and quality with heat pump operating temperature. Mass flow rate has to tendency to decrease with the rise of heat pump operating temperature. Besides, the pressure ratio increases from 4.61 to 5.25 and the compressor work decreases by 0.29% from 2.9 to 2.8. Generally, heat exchanging rate is reduced at the condenser with the rise of heat pump operating temperature. Thus, the temperature and pressure of refrigerant through the EEV are increased proportionally with the outlet temperature at the condenser. Therefore, the quality of refrigerant at the inlet of evaporator is increased. Furthermore, the entering pressure at the compressor inlet decreases and compressor work increases owing to the increase of pressure ratio between inlet and outlet of compressor. In this study, when the heat pump operating temperature increases from 40^{o}C to 48^{o}C, the condenser outlet temperature increases from 93.4^{o}C to 100^{o}C and quality increases from 0.321 to 0.379. Since heat pump operating temperature is very effective to system performance, the operator should control to maintain the optimal heat pump operating temperature according to operating condition in order to save energy and increase system reliability.

3.2The effect of ground temperature on system performance

Fig. 4 shows the variations of the optimal EEV opening, mass flow rate, heating capacity, and COP with ground temperature. The heating performance can improve as the ground temperature rises. As the ground temperature increases from 13^{o}C to 17^{o}C, the heating capacity is improved by 4.7% from 11.5 kW to 12.2 kW and the heating COP increases by 19% from 4.7 to 5.6. The temperature and pressure at the compressor inlet increases as the ground temperature elevates. At this case, the mass flow rate of refrigerant increases because of the high temperature and pressure. Hence, the optimal EEV opening increases with a rise of ground temperature. In this simulation result, the optimal EEV opening increase from 42% to 46% when the ground temperature increases from 13^{o}C to 17^{o}C. The mass flow rate of refrigerant is also increased from 68 g/s to 74 g/s.

Fig. 5 shows the variations of the compressor work, pressure ratio, evaporator outlet temperature and evaporator capacity with ground temperature. The compressor outlet temperature decreases with reduction of compressor pressure ratio when the ground temperature elevates. Since the evaporator is directly affected by the ground temperature, the pressure of compressor inlet increases, and the pressure ratio of a compressor reduces as the ground temperature rises. Besides, the compressor work decreases during compression process due to rise of compressor efficiency. Therefore, the system performance improves under the same indoor heating load condition with the increase of ground temperature. As the simulation result, the compressor pressure ratio is reduced from 5 to 4.6 and compressor work decreases from 2.9 to 2.8 kW when the ground temperature increases from 13^{o}C to 17^{o}C. The evaporator capacity increases by 7.7% from 9.0 to 9.7 kW and evaporator outlet temperature increases from 6.5^{o}C to 7.7^{o}C. From the simulation result, it can be deduced that the heating capacity can be maintained over the wanted heating capacity whole of winter season and system performance is also improved significantly by adapting the solar geothermal hybrid heat pump system.

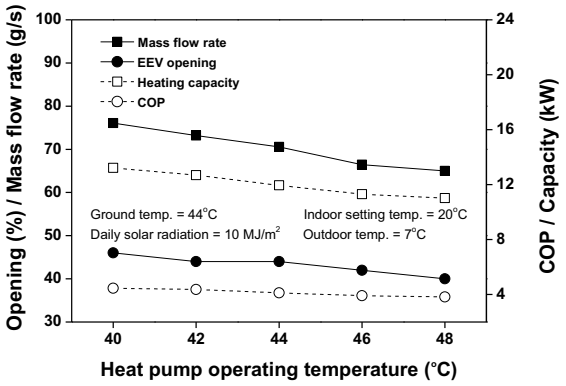

Fig. 2: Variations of optimal EEV opening. mass flow rate, COP and heating capacity with heat pump operating temperature.

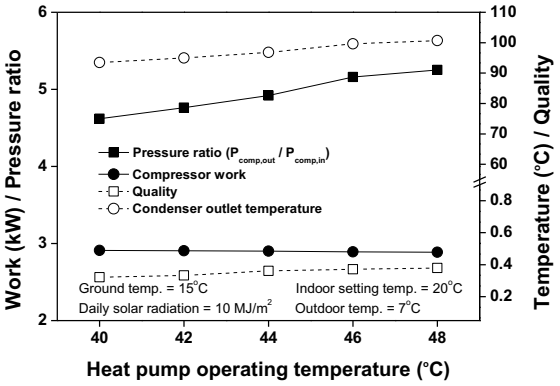

Fig. 3: Variations of compressor work, pressure ratio, quality and condenser outlet temperature with heat pump operating temperature.

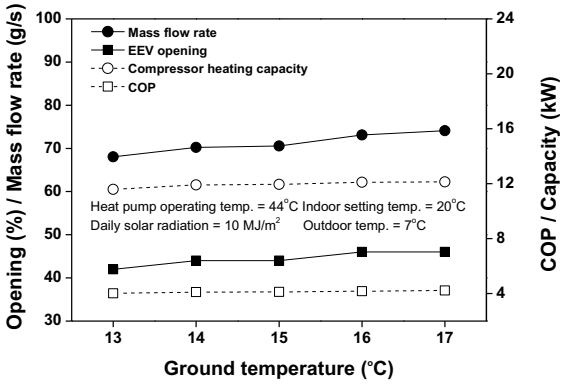

Fig. 4: Variations of optimal EEV opening, mass flow rate, COP and heating capacity with ground operating temperature.

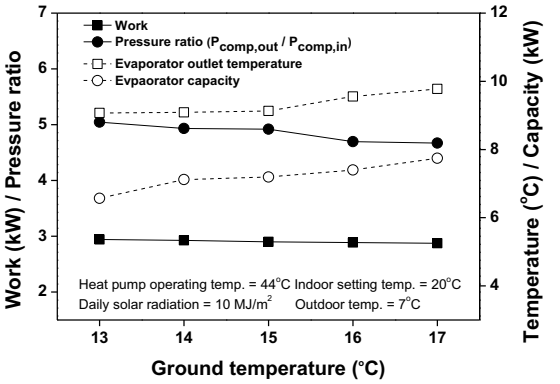

Fig. 5: Variations of compressor work, pressure ratio, evaporator outlet temperature, and evaporator capacity with ground operating temperature.

4. CONCLUSIONS

The simulation model of solar geothermal hybrid heat pump system (SG-HHPS) was developed to investigate system performance under variations condition. The performance characteristics of refrigerating system were analyzed with heat pump operating temperature and ground temperature. The results of numerical analysis was obtained through this study are followings.

When the heat pump operating temperature increase from 40 to 48°C, the optimal EEV opening decreases from 46% to 40%, and mass flow rate is also decreased from 76 g/s to 65 g/s. The heating capacity is linearly decreased from 13.2 kW to 11 kW. Besides, the heating COP decreases by 13.6% from 4.4 to 3.8. When the ground temperature increases from 13°C to 17°C, the heating capacity is improved by 4.7% from 11.5 kW to 12.2 kW and the heating COP increases by 19% from 4.7 to 5.6. Compressor pressure ratio is reduced from 5 to 4.6 and compressor work decreases from 2.9 to 2.8 kW. Besides, the evaporator capacity increases by 7.7% from 9.0 to 9.7 and evaporator outlet temperature increase from 6.5°C to 7.7°C. From the simulation result, it can be deduced that the heating capacity can be maintained over the wanted heating capacity and system performance is also improved significantly by adapting the solar geothermal hybrid heat pump system.

ACKNOWLEDGE

"This research was supported by Basic Science Research Program through the National Research Foundation of Korea(NRF) funded by the Ministry of Education, Science and Technology(2010-00-04369)"

References

ASHRAE, 1983, Methods of testing for seasonal efficiency of unitary air-conditioner and heat pumps, ASHRAE Standard 116.

Gnielinski, V,. 1976, New equations for heat and mass transfer in turbulent pipe and channel flow, International Chemical Engineering, Vol. 16, pp. 59-68.

Churchill, S. W., 1977, Friction-factor equation span all fluid flow regimes, Chemical Engineering, Vol. 7, pp. 91-92.

Shah, M. M,. 1979, A General Correlation for Heat Transfer during Film Condensation Inside PiPes, International Journal of Heat Mass Transfer, Vol. 22 pp. 547-665

Dittus, F. W., Boelter, L. M. K., 1985, Heat transfer in automobile radiators of the tubular type, International Communications in Heat and Mass Transfer, 12(1), pp. 3-22

Alireza Hobbi., Kamran Siddiqui., 2009, Optimal design of a forced circulation solar water heating system for a residential unit in cold climate using trnsys, Solar energy, Vol. 83, pp.700-714

X. Guoying., Z. Xiaosong., D .Shimnig., 2006. A simulation study on the operating performance of a solar-air Source heat pump water heater, Applied thermal engineering, Vol. 26, pp. 1257-1265

N. C. Baek., J. K. Lee., B. H. Song., 2001, Performance of Dual source Heat pump System with Solar-Assisted Evaporator, Proceeding of SAREK summer annual conference, pp.1334-1338

Y. C. Park., J. Y. Kim., G. S. Ko., 2007, A Study of Performance Characteristics on Hybrid Heat Pump System with Solar Energy as Heat Source, Journal of Korean Solar Energy Society, Vol. 27, No. 1, pp. 47-54